AD-A082 009 SACLANT ASW RESEARCH CENTRE LA SPEZIA (ITALY) F/G 20/1
THE AIM PROJECT: INTERVAL WAVES AND MICROSTRUCTURE IN THE THERM--ETC(U)
SEP 79 R B WILLIAMS
UNCLASSIFIED SACLANTCEN-SM-126 NL

END
DATE FILMED
4 80
DTIC

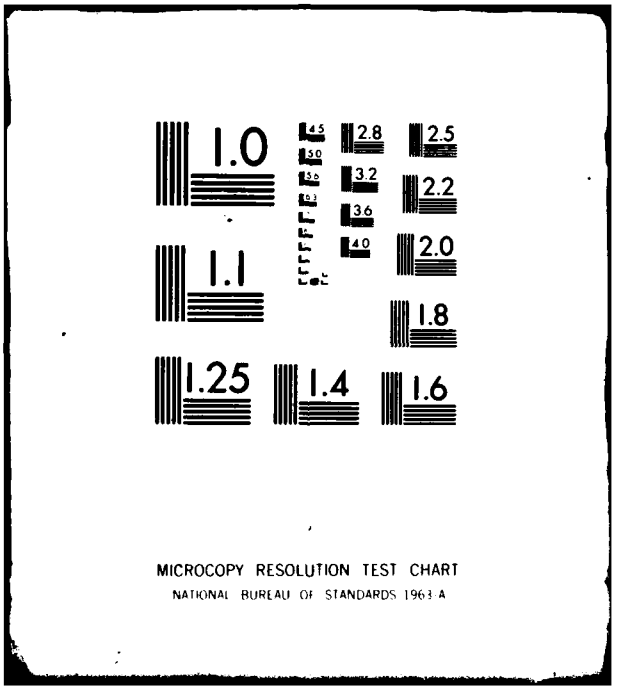
1.0
1.1
1.25
1.4
1.6
1.8
2.0
2.2
2.5
2.8
3.2
3.6
4.0
4.5
5.0
5.6
MICROCOPY RESOLUTION TEST CHART
NATIONAL BUREAU OF STANDARDS 1963-A

LEVEL

# SACLANT ASW RESEARCH CENTRE MEMORANDUM



## THE AIM PROJECT:
## INTERNAL WAVES AND MICROSTRUCTURE IN THE THERMOCLINE AND THEIR EFFECTS ON ACOUSTIC PROPAGATION

by

ROBERT B. WILLIAMS



15 SEPTEMBER 1979



NORTH ATLANTIC TREATY ORGANIZATION

LA SPEZIA, ITALY

*Published by*

[redacted]

| MINISTRIES OF DEFENCE | Copies |
|---|---|
| MOD Belgium | 2 |
| DND Canada | 10 |
| CHOD Denmark | 8 |
| MOD France | 6 |
| MOD Germany | 15 |
| MOD Greece | 11 |
| MOD Italy | 10 |
| MOD Netherlands | 12 |
| CHOD Norway | 10 |
| MOD Portugal | 5 |
| MOD Turkey | 5 |
| MOD U.K. | 16 |
| SECDEF U.S. | 61 |

| NATO AUTHORITIES | |
|---|---|
| Defence Planning Committee | 3 |
| NAMILCOM | 2 |
| SACLANT | 10 |
| SACLANTREPEUR | 1 |
| CINCWESTLANT/COMOCEANLANT | 1 |
| COMIBERLANT | 1 |
| CINCEASTLANT | 1 |
| COMSUBACLANT | 1 |
| COMMAIREASTLANT | 1 |
| SACEUR | 2 |
| CINCNORTH | 1 |
| CINCSOUTH | 1 |
| COMNAVSOUTH | 1 |
| COMSTRIKFORSOUTH | 1 |
| COMEDCENT | 1 |
| COMMARAIRMED | 1 |
| CINCHAN | 1 |

| SCNR FOR SACLANTCEN | |
|---|---|
| SCNR Belgium | 1 |
| SCNR Canada | 1 |
| SCNR Denmark | 1 |
| SCNR Germany | 1 |
| SCNR Greece | 1 |
| SCNR Italy | 1 |
| SCNR Netherlands | 1 |
| SCNR Norway | 1 |
| SCNR Portugal | 1 |
| SCNR Turkey | 1 |
| SCNR U.K. | 1 |
| SCNR U.S. | 2 |
| SECGEN Rep. | 1 |
| NAMILCOM Rep. | 1 |
| French Delegate | 1 |

| NATIONAL LIAISON OFFICERS | |
|---|---|
| NLO Canada | 1 |
| NLO Denmark | 1 |
| NLO Germany | 1 |
| NLO Italy | 1 |
| NLO U.K. | 1 |
| NLO U.S. | 1 |

| NLR TO SACLANT | |
|---|---|
| NLR Belgium | 1 |
| NLR Canada | 1 |
| NLR Germany | 1 |
| NLR Greece | 1 |
| NLR Italy | 1 |
| NLR Norway | 1 |
| NLR Portugal | 1 |
| NLR Turkey | 1 |

| | |
|---|---|
| Total initial distribution | [redacted] |
| SACLANTCEN Library | [redacted] |
| Stock | [redacted] |
| Total number of copies | [redacted] |

(14) SACLANTCEN [redacted]-SM-126

NORTH ATLANTIC TREATY ORGANIZATION

SACLANT ASW Research Centre
Viale San Bartolomeo 400, I-19026 San Bartolomeo (SP), Italy.

tel: national 0187 503540
international + 39 187 503540

telex: 271148 SACENT I

(9) Memorandum rept.,

(6) THE AIM PROJECT:
INTERNAL WAVES AND MICROSTRUCTURE IN THE THERMOCLINE
AND THEIR EFFECTS ON ACOUSTIC PROPAGATION.

by

(10) Robert Bruce Williams

(11) 15 Sep[redacted]979

(12) 30



This memorandum has been prepared within the SACLANTCEN Underwater Research Division as part of Project 04.

G.C. VETTORI
Division Chief

312950

## TABLE OF CONTENTS



## List of Figures

# THE AIM PROJECT: INTERNAL WAVES AND MICROSTRUCTURE IN THE THERMOCLINE AND THEIR EFFECTS ON ACOUSTIC PROPAGATION

by

Robert Bruce Williams

## ABSTRACT

*A coordinated set of three experiments was performed in the Gulf of Lions in September 1976 to study physical processes in the thermocline and their effects on acoustic propagation. Simultaneous measurements from two ships and three bottom-moored buoy systems were made of such oceanographic parameters as temperature, salinity, and current velocity so as to assess internal wave motions, advecting features of temperature and salinity irregularities, vertical microstructure of temperature and salinity, and turbulence. In addition, a concurrent acoustic propagation experiment in the 3 to 12 kHz band was conducted over a range of 3 to 10 km to assess multipath arrival characteristics and to measure phase and amplitude fluctuations along a single path. Signals were received on a five-element vertical array, from which vertical angles of arrival could be derived for the different paths. Oceanographic results were: (1) analysis of vertical displacements of pycnoclines and thermoclines from a towed instrument and a continuously-profiling microstructure instrument produced vertical and horizontal spectra that are compared with recent internal-wave models; (2) 14-day current meter records above and below the thermocline from a subsurface mooring show rather large inertial energy (18-h period) attenuating rapidly with depth, and internal-wave energy for shorter periods; (3) parameters that characterize the turbulence at small scales, such as the rates of dissipation of kinetic energy and temperature variance, and the diffusion coefficients were deduced from the temperature, conductivity, and current records of a microstructure instrument. Acoustic results were: (1) large numbers of multiple arrivals were observed, even at the shorter ranges, with a time spread of usually less than 2 ms, but at times as much as 5 ms; (2) large (>20 dB) fluctuations in amplitude were found for a given ray; (3) amplitude spectral analysis showed rapid cutoff of amplitude fluctuations for periods shorter than 2 min, corresponding to range changes of 35 m.*

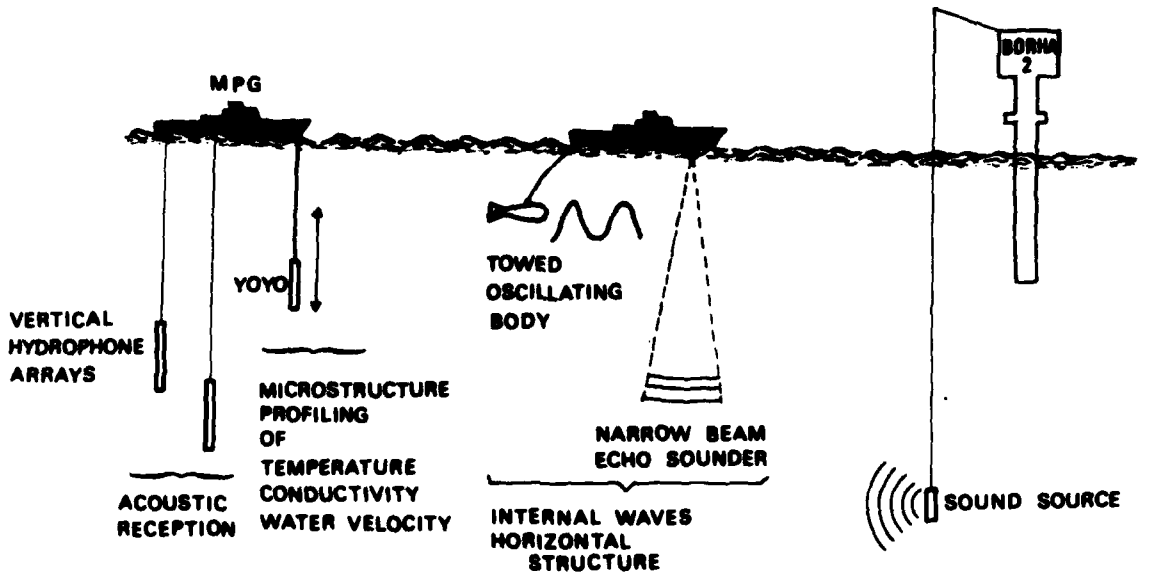


*FIG. 1 AIM EXPERIMENTS*

## INTRODUCTION

As part of SACLANTCEN's oceanic variability studies, the AIM project was initiated to investigate in detail the physical causes of fluctuations and distortions of sound propagating in and directly below the thermocline. It is thought that the largest fluctuations and distortions of sound in the sea occur in the thermocline, due to the large sound-speed variability found there. A knowledge of the characteristics of the fluctuations, and how these fluctuations are manifested, would not only aid in predicting sonar performance, but also help in designing new sonar systems, and possibly even suggest certain oceanic regions of peculiarly high or low acoustic variability.

A sea trial, consisting of three concurrent experiments, was conducted in September 1976 about 60 n.mi offshore in the Gulf of Lions in the Mediterranean. Some of the oceanographic aspects of the sea trial were a part of COBLAMED 1976, an international oceanographic programme organized by France and sponsored by the NATO Scientific Affairs Division to study large-scale responses of the sea to mistral wind conditions; i.e., gale-force winds from the north. The AIM operation took place when these strong winds were absent, although it had to be temporarily stopped at times due to rough seas caused by the onset of the mistral.

The three experiments that comprised the AIM study were as follows:

1. A spatial and temporal study of internal gravity waves and horizontally-advecting irregularities or "blobs".
2. A study of the dynamics of small-scale or microstructure processes.
3. Acoustic propagation studies over ranges of 3 to 10 km at 3 to 12 kHz frequencies.

Experiments reported in the literature have usually examined only one of these three aspects. Although a great deal of effort is required to perform all three simultaneously, there is much to be gained by doing so: the relationship between internal waves and microstructure is not yet well understood, and the roles that microstructure and internal waves play in causing fluctuations and distortions of acoustic signals needs much work. The intent of this project was to add to our understanding of both these interactions as well as adding to the knowledge of the three aspects individually.

## 1 THREE SIMULTANEOUS EXPERIMENTS

### 1.1 Experiment 1: Internal Gravity Waves and Blobs

Contributions to sound-speed fluctuations are (a) gravity waves internal to the sea and (b) horizontal irregularities (blobs) carried in space by currents. The experiment aimed at describing the characteristics of both these phenomena.

Early in the century, by sampling water at various depths, oceanographic researchers detected fluctuations in the vertical structure of temperature and salinity, and speculated that these could be due to gravity waves propagating internally. The development of the bathythermograph (BT) in 1940 vastly extended the sampling resolution both in time and space, with consequent observations of energy at higher frequencies and of smaller scales. Although a few observations and some speculations were put forth during the first half of the century, a rapid increase in research on internal waves has taken place only in the last decade. The now classic paper of Garrett and Munk *[1]* (hereafter referred to as *GM72*) has greatly advanced the field. This paper set down the governing equations of the physics and constructed a set of semi-empirical models for the time and space statistics that were consistent with most of the observations at that time. Since then, most researchers have referred to this paper to compare and to contrast their observations and theories. The large amount of recent activity motivated a special collection of reprints issued by the *Journal of Geophysical Research* in 1975. Briscoe *[2]* undertook the task of summarizing the vast amount of work from 1971 to 1975, and provided an extensive bibliography.

In *GM72*, the power spectrum of the vertical wavenumber, $\beta$, of the vertical displacement, $\zeta$, of isopotential density surfaces, is given as

$$F(\beta) = \text{const. for } \beta < \beta \text{ crit}$$
$$= 0 \qquad \beta > \beta \text{ crit} \qquad \text{[Eq. 1]}$$

The spectrum of horizontal wavenumber, $\alpha$, is given as

$$F(\alpha) \propto (\alpha)^{-2} \qquad \text{[Eq. 2]}$$

for an intermediate band of horizontal wave numbers, $\alpha$, and zero above $\alpha$ crit. A revised model by the same authors in 1975 *[3]*, hereafter referred to as *GM75*, based on recent data puts

$$F(\beta) \propto (\beta)^{-5/2}$$

and

$$F(\alpha) \propto (\alpha)^{-5/2}$$

for $\alpha$ and $\beta$ large. In their paper, however, they stress that a precise determination of the internal wave spectra at high wave numbers remains a problem of great importance. One of the aims in the reported study was to make measurements that yield good estimates of $F(\alpha)$ and $F(\beta)$ simultaneously, reducing as much as possible the influences of blobs and vertical fine structure (see experiment 2 in Sect. 1.2).

The ocean can be pictured, in the absence of internal waves and currents, as having horizontal irregularities of temperature and salinity, which we call blobs. Since there are no horizontal forces in such a situation, there are no horizontal density gradients, and the horizontal changes in temperature are accompanied by changes in salinity that keep the density constant. Introduction of internal waves will cause vertical displacements of the blobs, but along an isopotential density surface the blobs

can still be described by irregularities in potential temperature and salinity. A further aim of this experiment was to estimate how much of the fluctuations in temperature could be assigned to internal waves and how much to blobs.

## 1.2 Experiment 2: Microstructure and Turbulence

Small irregularities of temperature, and sometimes of salinity, are nearly always found in the thermocline. These irregularities,or fine structure, usually tend to form vertical, step-like shapes of fairly constant temperature layers accompanied by thin regions or sheets of rapidly changing temperature between the layers. The generation and degeneration of these features have been of much interest to the oceanographic community for some time (see, for example, *[4]*). A discussion by Garrett and Munk of the relationship between internal waves, fine structure, and turbulence can be found in *[5]*, based on their internal wave model *GM72*.

Parameterization is needed to describe turbulence phenomena, thereby requiring estimates of the values of the parameters. A discussion of turbulence and turbulence parameters in the thermocline of the ocean can be found in *[6]* and *[7]*. Two important turbulence parameters are $\varepsilon$, the rate of dissipation of kinetic energy, and $\chi$, the rate of dissipation of temperature variance. Estimates of these parameters can be obtained from data provided by a vertically-profiling microstructure system. To date very few estimates of turbulence parameters have been put forward in the literature, and of these, many are in dispute. Our hope was to add to the data base of turbulence information and, because internal waves were concurrently measured, to be able to draw inferrences as to their interactions.

## 1.3 Experiment 3: Acoustic Propagation

For many years, acoustic fluctuation studies in the ocean have applied homogeneous turbulence theories of the medium *[8, 9]* to predict statistics of phase and amplitude fluctuations. However, except for perhaps the surface mixed layer, these have usually failed due to the facts that (a) the ocean is vertically stratified and therefore not homogeneous and (b) most of the fluctuations in sound speed are caused by propagating internal waves. With the large increase in ability to describe internal waves (see Sect. 1.1), formalisms of the effects of internal waves on acoustic transmission are appearing in the literature *[10, 11, 12]*. Although these models ignore fine structure and turbulence, for acoustic frequencies below 1 kHz and long ranges (>100 km) there is reasonable agreement between data and predictions.

However, at the higher frequencies and shorter ranges it is not clear whether or not these smaller scale oceanic processes play a major or even dominant role in causing acoustic fluctuations. A goal of the present experiment was the description and characterization of the received acoustic signals. These data, together with the concurrently collected data of experiment 1 (internal waves and blobs) and experiment 2 (microstructure and turbulence) form a basis for assessing the roles that these physical processes play in the distortion of sound.

## 2 EXPERIMENTAL SETUP AND EQUIPMENT

Figure 1 depicts the physical arrangements of the experiments. A sound source deployed on the French moored buoy BOHRA II emitted short (0.4 ms) pulses containing energy in the 3 to 12 kHz frequency band once per second. The actual signal transmitted is shown in Fig. 2a. The signal of the 4 kW (peak) source was generated by discharging a high-voltage capacitor through the transducer. Reception took place on SACLANTCEN's MARIA PAOLINA G., positioned 3 to 10 km away, on one of two vertical arrays composed of five hydrophones spaced 40 cm apart. The hydrophones themselves were 1/2 in. (12.7 mm) diameter spheres, placed in a 1 in. (25.4 mm) diameter clear plastic tube filled with a semi-rigid plastic within which were three very small (1 mm diameter) load-bearing wires. Extreme care was taken in their construction so that the structure of the array itself would not produce any appreciable phase shifts.

Data collection of the received pulses was synchronized by the previous pulse, so that sampling started about 1 ms before the beginning of the various arrivals. Digitization and recording of each of the five hydrophone signals, after amplification, was done with a Hewlett-Packard minicomputer system. The digitization period was 4 or 8 ms (depending on the run) at a sampling rate of 48 kHz. Real-time processing included a display of a selected digitized signal, together with cross-correlation processing and display of any pair of hydrophone signals. A pressure gauge on each hydrophone array measured depth to a relative accuracy of 7 cm.

The naval hydrographic ship MAGNAGHI (IT) was used to tow the Centre's towed oscillating body (TOB) *[13]*, instrumented with Plessey CTD sensors and electronics, and a current meter. Figure 3 shows the TOB and its operation, in which a winch vertically oscillates a light-weight instrumented package along a weighted support cable. A second Hewlett-Packard minicomputer system digitized and logged the data. The real-time processing consisted of time plots of isotherm or isodensity surfaces.

Various tows at about 2 kn were done by the MAGNAGHI over several days in several different directions. The TOB oscillated from 20 to 70 m depth, covering the bottom of the mixed layer and the top of the thermocline. On board the MAGNAGHI the 30 kHz gyro-stabilized, narrow-beam (3°) echo sounder was used with a pulse width of 1 ms to examine the thermocline structure. Comparison with XBT and TOB records taken at the same time demonstrated that this instrument is capable of detecting and measuring the depth of strong thermal-gradient regions. Thus the echo sounder could be used to observe vertical fluctuations of the thermocline structure while the ship was cruising at 10 kn, as well as at 2 kn when towing the TOB.

For the microstructure studies, as well as for the internal wave work, a vertical microstructure-profiling system was deployed from the MARIA PAOLINA, as depicted in Fig. 1. A computer-controlled winch raised and lowered the microstructure package, which consisted of a Neil Brown conductivity/temperature/depth (CTD) instrument, a two-axis Crouzet acoustic horizontal current meter, a magnetic compass, and two horizontal

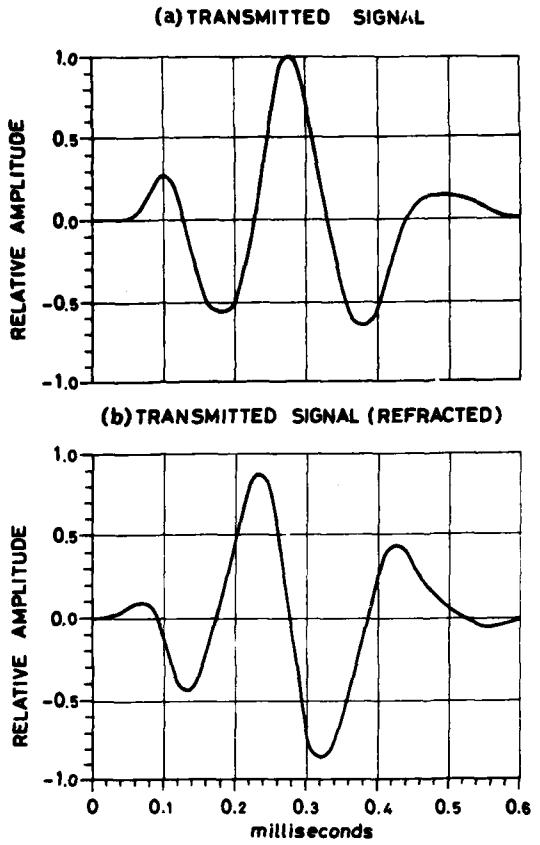


*FIG. 2 TRANSMITTED SIGNAL*

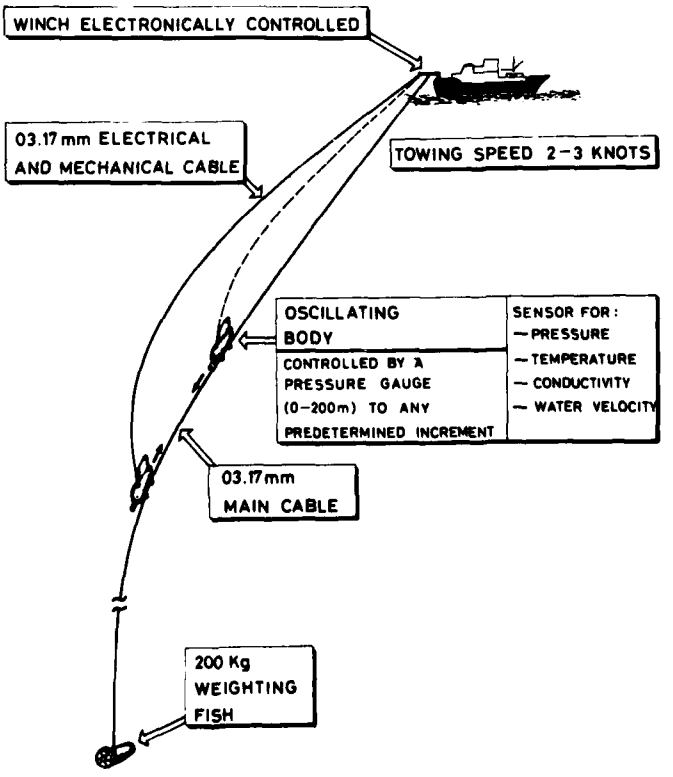


*FIG. 3 TOWED OSCILLATING BODY (TOB)*

accelerometers. The signals were digitized in the fish, and the multiplexed signals were sent by cable to a deck unit for monitoring and to a third Hewlett-Packard minicomputer system for data logging and real-time processing of selected signals. This processing included displays of sensor profiles, as well as of profiles of calculated variables such as density, Väisälä-Brunt frequency, and Richardson number.

During the experiment, the MARIA PAOLINA drifted away from BOHRA II (the acoustic source), at a rate of 0.5 to 1.5 kn. A profile was usually taken every 2 min at a lowering speed of 50 cm/s, and typically a run lasted 5 to 6 hours, covering a distance of about 7 to 8 km. Over one thousand profiles were taken during the study. The data provided horizontal and vertical wave-number spectra of vertical height fluctuations of density surfaces, such as would be caused by propagating internal waves. Additionally, details of the vertical density structure, the current shear, and small-scale fluctuations of sound speed and temperature could be obtained.

A subsurface mooring near BOHRA II was laid on the bottom at 2300 m, with the uppermost float at a depth of 25 m. Two Aanderaa current meters, one in the mixed layer at 30 m depth, and the other in the base of the thermocline at a depth of 75 m, yielded current and temperature records for a two-week period.

## 3 DATA AND DISCUSSION

### 3.1 Mooring Data

The two weeks of current meter records have been spectrally analyzed for clockwise and counterclockwise motions, in the same manner as used by Perkins *[13]*. Figure 4 is the result of seven frequency spectral averages, each of about 42 hours duration, for the time series recorded at 75 m depth. Comparison of the data with internal wave models is given in Section 3.5.

Due to the success of using *GM72* and *GM75*, the Mediterranean data of Perkins were reexamined. A fit to the model was made to these (six-week) spectra for the five depths. The level $Eb^2No$ was found to be a factor of 2 to 10 below the level estimated by *GM72*, and there was also a strong suggestion of a reduction in this energy level away from the surface and bottom boundaries. In addition, the form of midwater records (700 to 1700 m) fits better to the *GM72* model than do the near-surface (200 m) or the near-bottom (2200 m) records. The data from the current meter also indicate a significantly lower energy level than the *GM72* value.

The energy of the inertial component for the 75 m depth is a factor of 28 below that of the mixed layer, while the average current for the 75 m depth was a factor of only 2 below the mixed-layer value. The vertical shear is therefore dominated by inertial energy. Figure 5 shows the progressive vector diagrams for the two current meters.

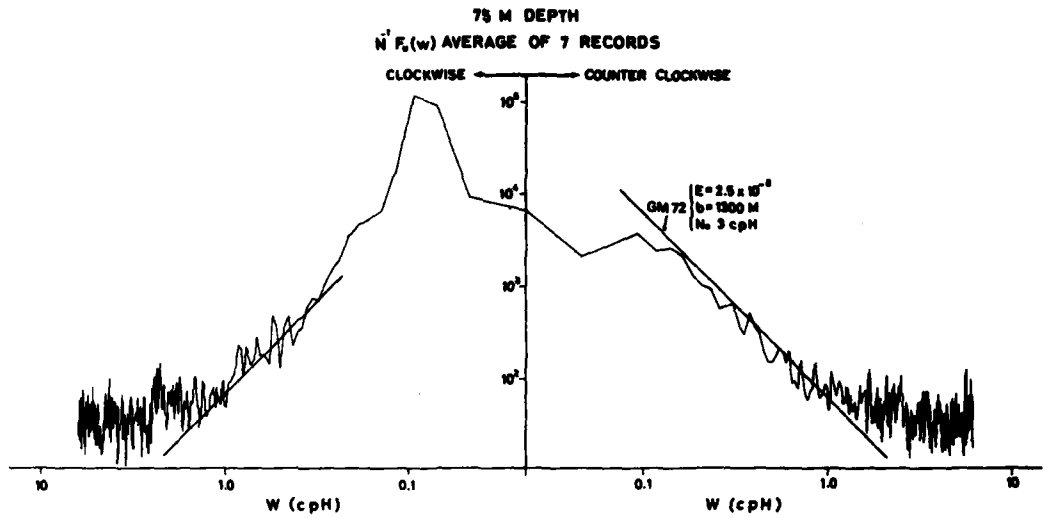


*FIG. 4 FREQUENCY SPECTRAL ANALYSIS OF CURRENT METER DATA*

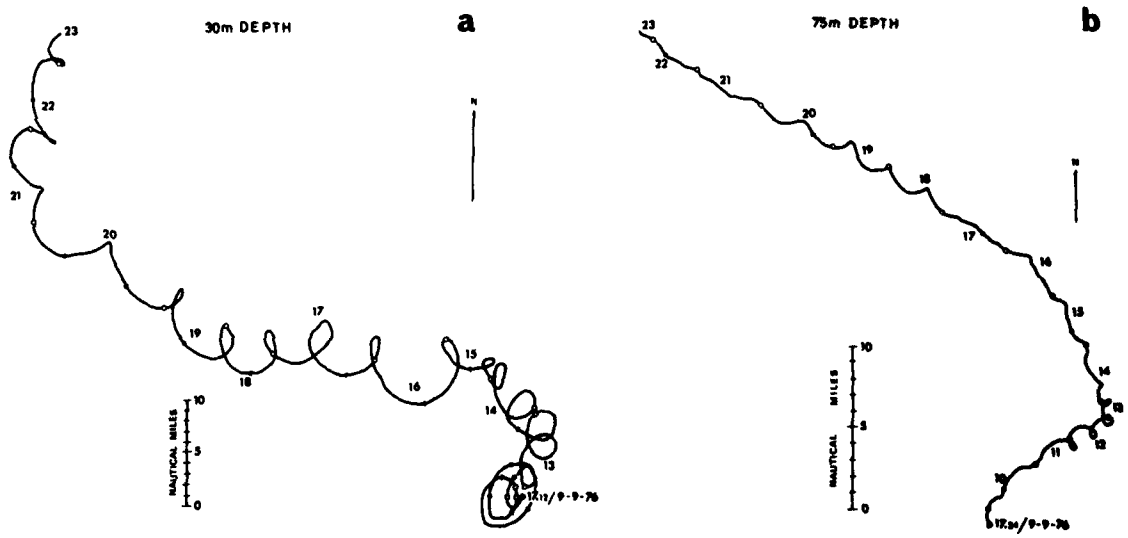


*FIG. 5 PROGRESSIVE VECTOR DIAGRAMS OF CURRENT METERS*

*(a) 30 m Depth*

*(b) 75 m Depth*

## 3.2 TOB Data

Isotherms from the TOB runs 2 (to the north) and 3 (to the south) are shown in Fig. 6, indicating two high temperature gradient regions near 30 and 55 m depths. This double gradient feature was prevalent throughout our experiments and is in evidence also in the data from the XBT, the narrow-beam echo sounder, and the microstructure-profiling system. The temperature-profile space structure of run 10 is shown in Fig. 7, along with symbols at prescribed temperatures. From our data, as well as from other observations made in this area, the entire thermocline is seen to participate in large vertical motions. There is no evidence to support the concept that the top of the thermocline might be a nodal point for internal waves.

The TOB instrument, as mentioned in Chapter 2, is also equipped with a conductivity sensor to allow salinity to be measured, which thereby allows the density to be calculated. However, as evidenced by the microstructure-system profiles, the salinity profiles at these depths show relatively small variations, and therefore the temperature changes alone are sufficient to indicate the density fluctuations.

To reduce the effects of fine structure (for a discussion see *[1]*), we have spectrally analyzed vertical height variations of isotemperature (or isodensity) surfaces — as opposed to spectral analyzing temperature fluctuations at a constant depth — and then divided the spectra by the average temperature gradient. The average power spectra for data from both a 'test' trial in October 1975 and the actual experiment in 1976 are shown in Fig. 8. There is no significant difference between the 1975 and the 1976 spectra.

## 3.3 Narrow-Beam Echo Sounder

Records of the acoustic returns of the echo sounder, interpreted as spatial views of the thermal structure, are shown in Figs. 9 and 10. In Fig. 9 the data from both the 10 kn and 2 kn runs show the two high temperature gradients. Excellent correspondence was obtained between the structures shown by these records and the regions of high temperature gradients shown by the XBT data (usually taken every 15 minutes) and the TOB data. The upper strip apparently shows the biological scattering layer rising towards the surface from about midpoint in the record. Also, due to the short pulse length used (1 ms), fine structure can be perceived within the strong gradients. These smaller features usually compare well with the XBT data. A rough estimate was made of the strength of the returns, and this was found to be consistent with being caused by reflections from the measured thermal gradients; i.e. it was not necessary to postulate biological scattering to explain the observed reflections.

Although the scattering layer during the night partially obscured some of the records, a striking set of features was observed (Fig. 10), accompanied by a drastically-changed temperature profile: profiles of XBTs 16, 17, and 18 indicate a change from a fairly uniform thermal gradient to a very sharp thermocline. Such an event, seen on the echo-sounder trace between times when XBTs were taken, indicates large vertical motion. The horizontal extent of any one of these events is

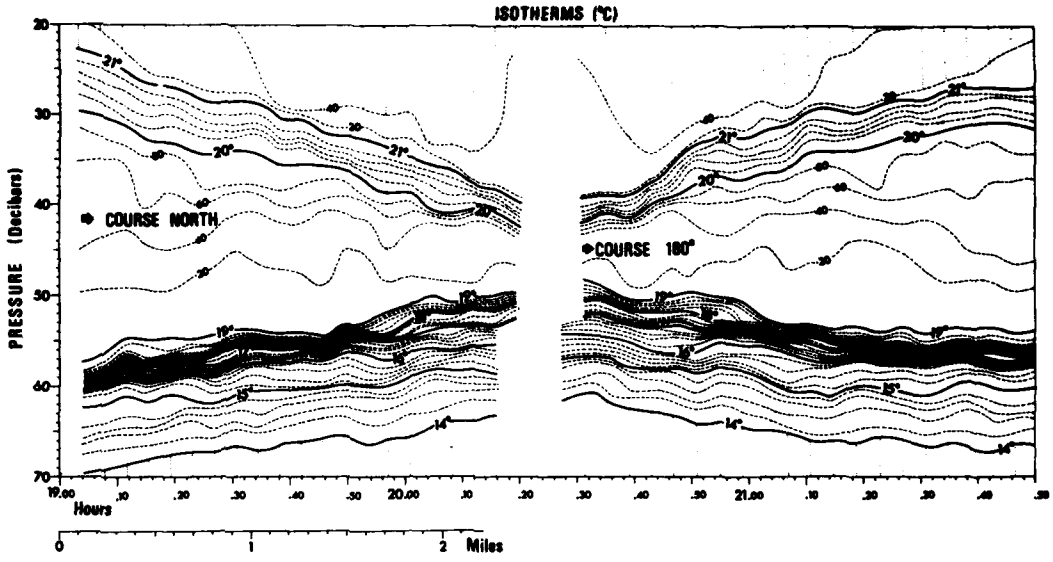


*FIG. 6 TOB TEMPERATURE DATA*

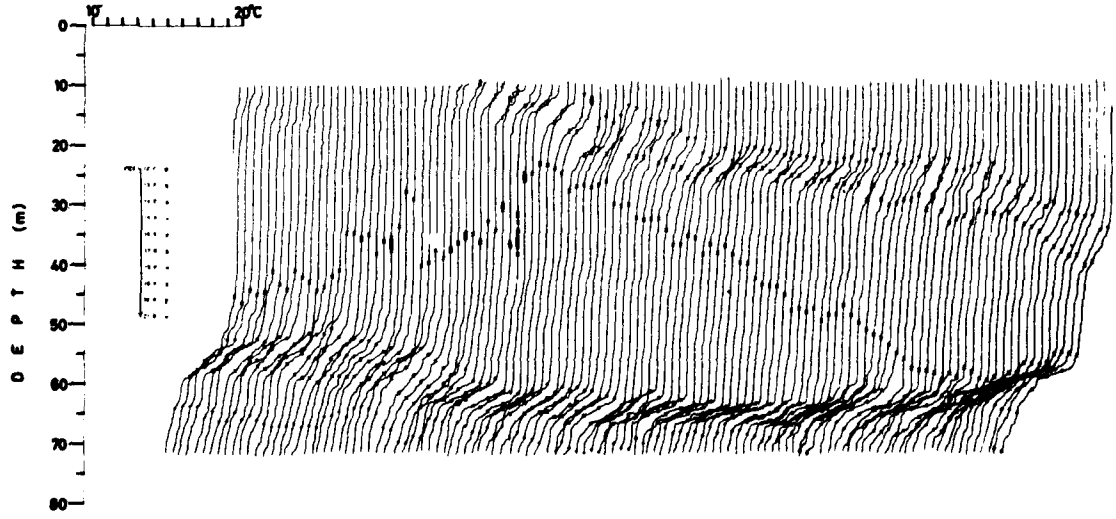


*FIG. 7 TOB RUN 10: TEMPERATURE SPACE STRUCTURE*

a

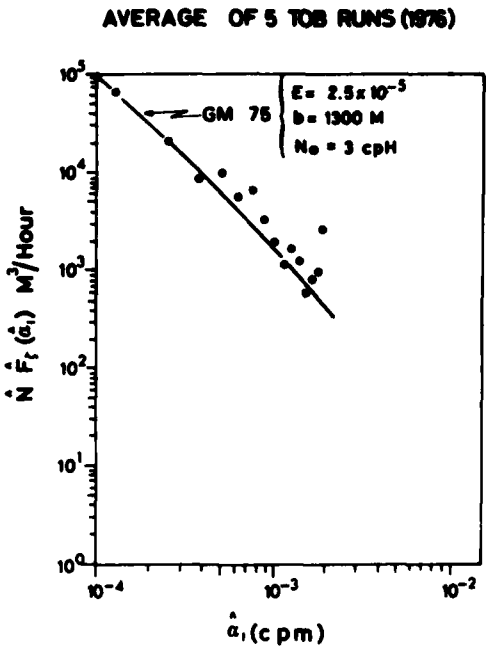


b

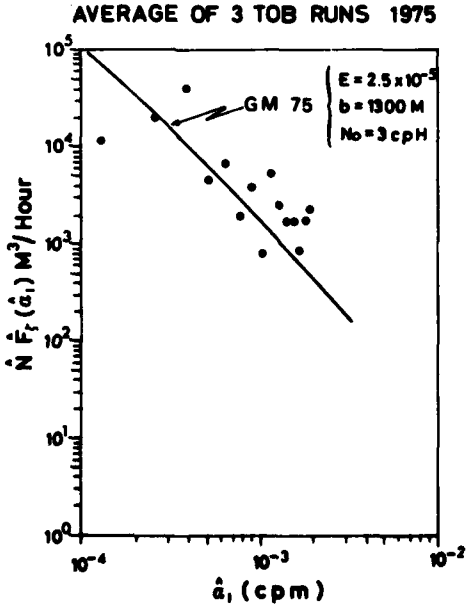


*FIG. 8 POWER SPECTRAL ANALYSES OF VERTICAL HEIGHT VARIATIONS OF ISOTEMPERATURE SURFACES*

*(a) Average of 5 TOB runs (1976)*

*(b) Average of 3 TOB runs (1975).*

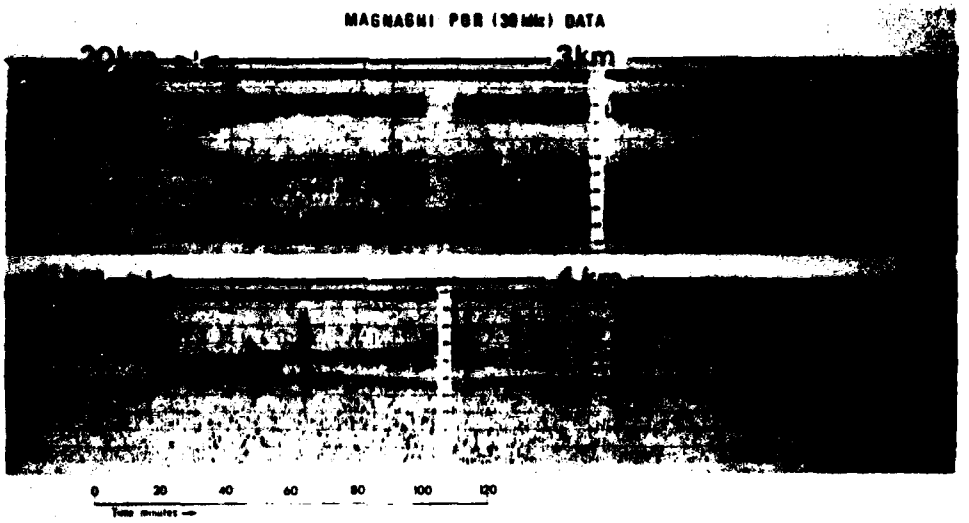


*FIG. 9 THERMAL STRUCTURES RECORDED BY ECHO SOUNDER*

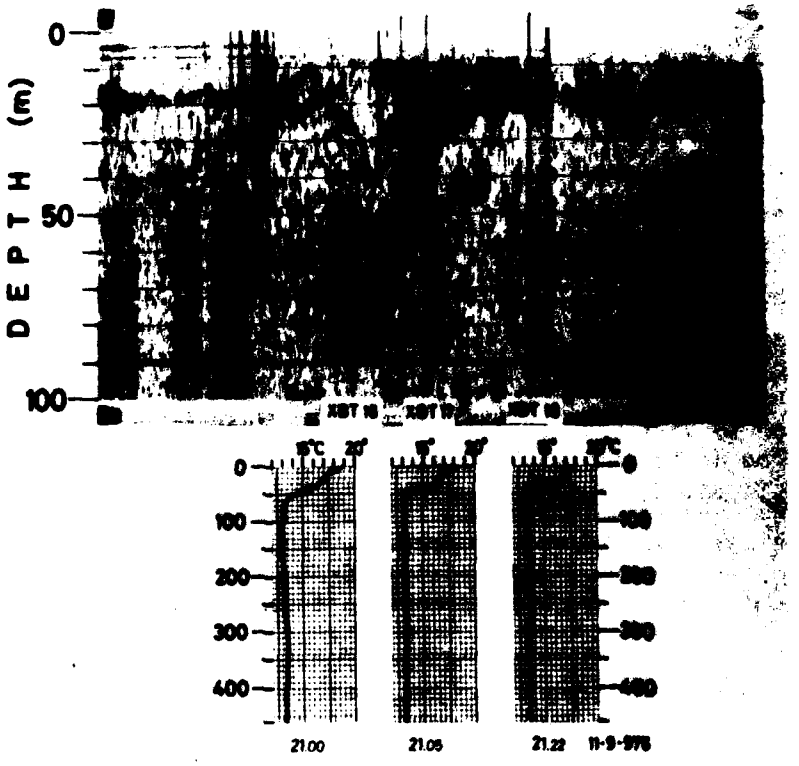


*FIG. 10 LARGE VERTICAL TEMPERATURE CHANGES WITHIN 70 m, AS RECORDED BY XBT AND ECHO SOUNDER*

about 70 m. This group of events was the only one observed during our experiments. The patterns are similar to laboratory-generated solitary waves.

### 3.4 Microstructure Profiling Data

Because of the large number of profiles taken, and also because of the precision and the fine-scale resolution of the instrument, high-quality statistics, such as horizontal and vertical spectra of various quantities, could be obtained. The following processing was done in order to obtain horizontal and vertical wavenumber spectra of fluctuations of isopotential density surfaces. An equally incremented set of standard values of isopotential density was assigned:

$$\rho(\text{standard}) = \rho \text{ initial} + (i-1) \times \delta\rho \qquad \text{[Eq. 3]}$$

$$\text{for } i=1,\ldots,n,$$

where $\rho$ initial, n, and $\delta\rho$ varied for different processing studies but typically n=128, $\rho$ initial = 1.028 and $\delta\rho = 3.4 \times 10^{-6}$ g/cm$^3$. Densities from the actual profile collected were calculated and, when two measured densities bracketed a standard density, a linearly-interpolated depth was assigned to the standard density. This depth was based on the two measured depths and the two densities derived from measured values. Thus, for each measured profile, a series of n depths (or vertical heights, $\zeta$) was created. For this processing, measured density inversions were ignored.

These height variations, $\zeta$, were spectral analyzed for each profile as a function of density; a typical spectrum averaged over 128 profiles is given in Fig. 11. Although the independent variable was density, conversion to a vertical wavenumber spectrum was made, based on the average density gradient. The large number of degrees of freedom, due to the large number of profiles processed, yielded good estimates of the spectrum, and can distinguish between the models of *GM75* and of Cairns and Williams *[15]*, as will be discussed in Sect. 3.5. Departure from the high wavenumber portion of *GM75* is noted at about 3 cycle/m into a $\beta^{-5/3}$ region.

In addition to vertical spectra, horizontal spectra of $\zeta$ have been derived from different profiles at a given standard density. Using the ship's drift speed, as obtained by radar fixes on BOHRA II, conversion was made to spatial coordinates. Sample spectra appear in Fig. 12, and agree well with the TOB data. However, finer horizontal spatial resolution is obtained for the microstructure system, and departures from the measured data from the *GM75* model are observed at the higher wavenumbers.

To ascertain the relative importances of blobs and internal waves, the following analysis was carried out. The series of $\zeta$, both horizontal and vertical, and their power spectra as described above, were compared with the results obtained when the same data processed by using standard densities for reference, instead of using standard potential temperatures. The results obtained by the two methods were identical, within expected

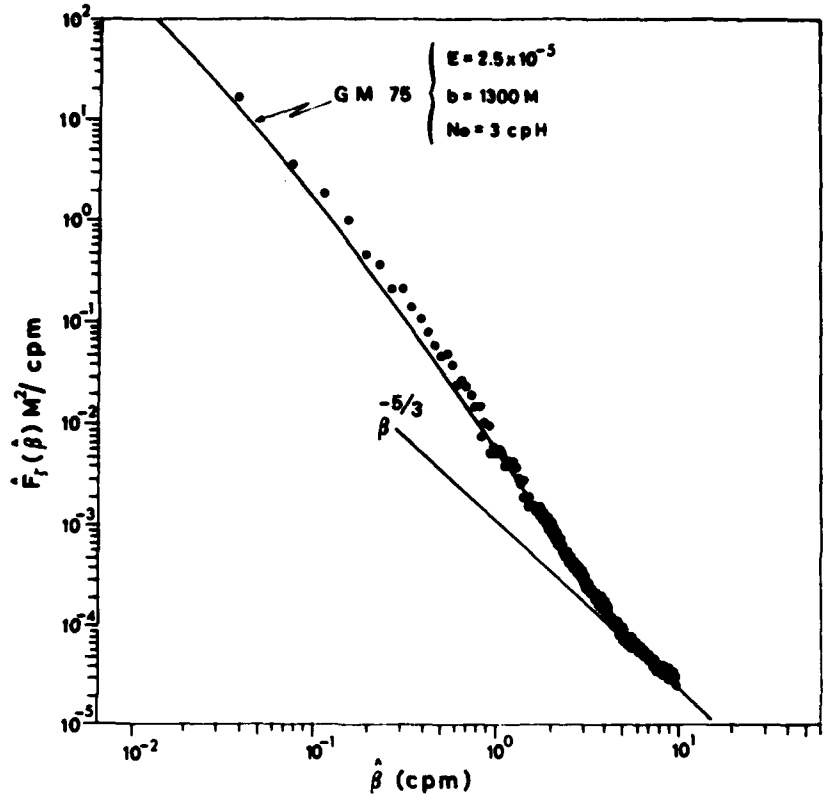


*FIG. 11 SPECTRAL ANALYSIS OF 120 VERTICAL TEMPERATURE PROFILES*

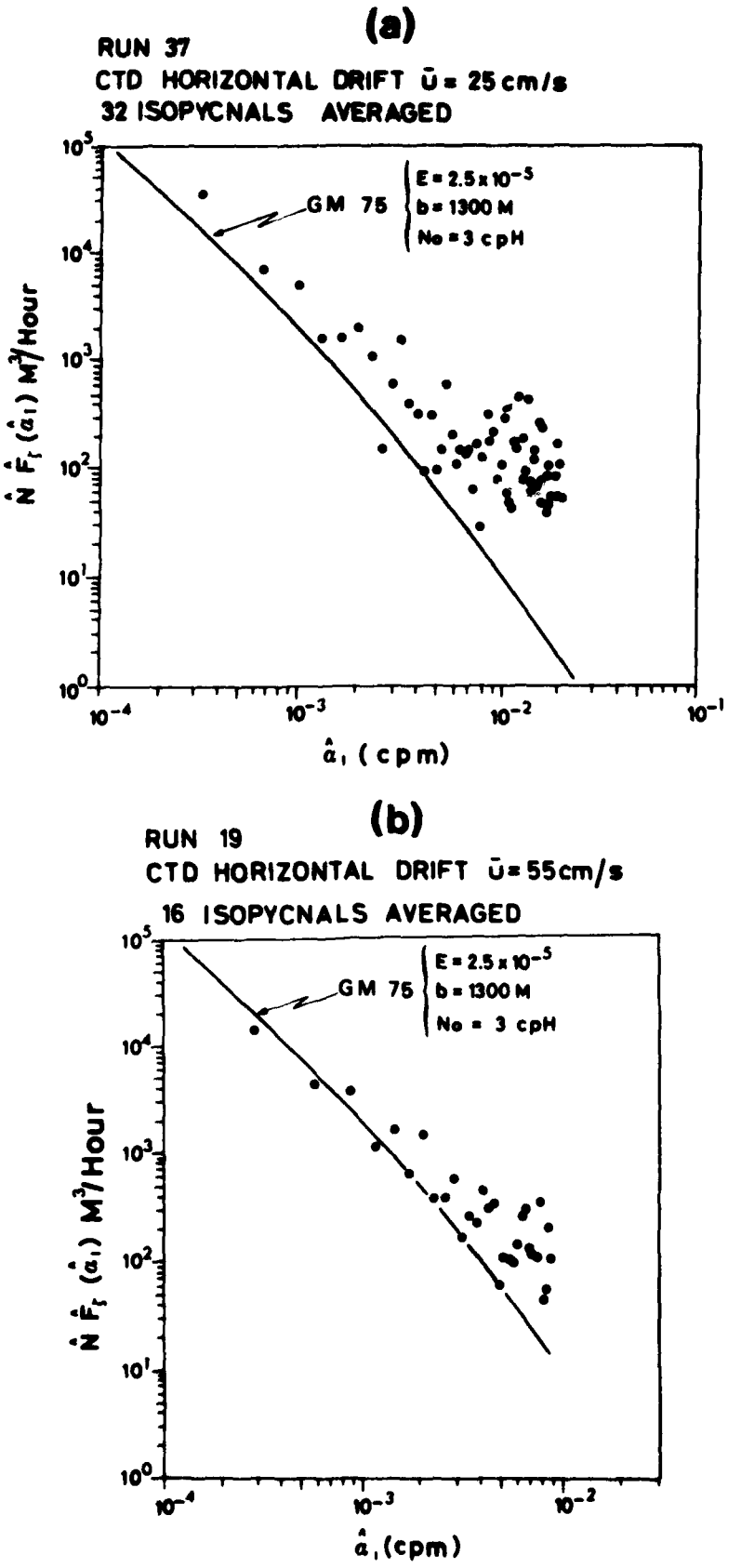


*FIG. 12 SPECTRAL ANALYSIS OF HORIZONTAL TEMPERATURE CHANGES*

*(a) Run 37 (b) Run 19*

statistical error, at all scales analyzed. It is concluded that, for our experimental setting, blobs were not a contributor to the variability within the thermocline, but that internal waves were. This result is certainly not expected to be universal, however. In the region of boundaries of two water masses, such as fronts, blobs could very well play a dominant role.

Figure 13 shows a typical temperature profile together with a blow-up of the fine structure. Figure 14 displays a portion of a profile series, indicating the downward motion (at that time) of the whole temperature structure, and also showing the two regions of high temperature gradients mentioned earlier. During event 181 an unusually large irregularity in temperature between 67 m and 69 m appears to be a mixing event. The blow-up shows the density structure, and indicates instabilities over 50 to 100 cm regions. Examination of the current-meter record for that time show fluctuations in horizontal velocities of about 2 to 3 cm/s that may have been associated with these irregularities. A rough estimate can be made of the rate of dissipation of kinetic energy, $\varepsilon$, by

$$\varepsilon = [(\delta u)^3]/(kL), \qquad \text{[Eq. 4]}$$

where $\delta u$ is the velocity difference across length L, and k is Von Karman's constant (0.40). This results in a large value of $\varepsilon$ of about 0.5 $cm^2\ s^{-3}$ for this event. Although this one event is perhaps most striking, other such events appear in the profiles during perhaps 1 to 2% of the time.

The current-meter data were spectral analyzed for different depths and different horizontal sections of water. It is believed that the band of frequencies above 0.2 Hz and below 0.8 Hz is relatively free from package motion. If this is not so, then turbulence parameters derived from these data should be regarded as upper limits to the actual values. A fit to the theoretical spectrum was made in this band. A typical spectrum appears in Fig. 15. The average value of $\varepsilon$ for this box of water from 66 to 82 m depth and 1380 m in horizontal extent is $1.28 \times 10^{-2}$, or about 2% of the aforementioned event. This suggests that the average value can be accounted for by events occurring during a small percentage of the time, i.e. that the turbulent field is intermittent.

### 3.5 Internal-Wave Spectra and the Garrett-Munk Model

Because these Mediterranean data were collected simultaneously from moored current meters, horizontally-towed sensors, and vertically-profiling sensors, a fairly complete comparison of them can be made with the *GM72* and *GM75* Garrett-Munk models. Their three scaling parameters are:

b = the vertical stratification scale

No = the vertical stability or buoyancy frequency scale

E = the dimensionless energy scale

and are compatible with the assumption of an exponentially-stratified ocean represented by the Väisälä-Brunt frequency profile as:

$$N(z) = No \times e^{(-z/b)} . \qquad \text{[Eq. 5]}$$

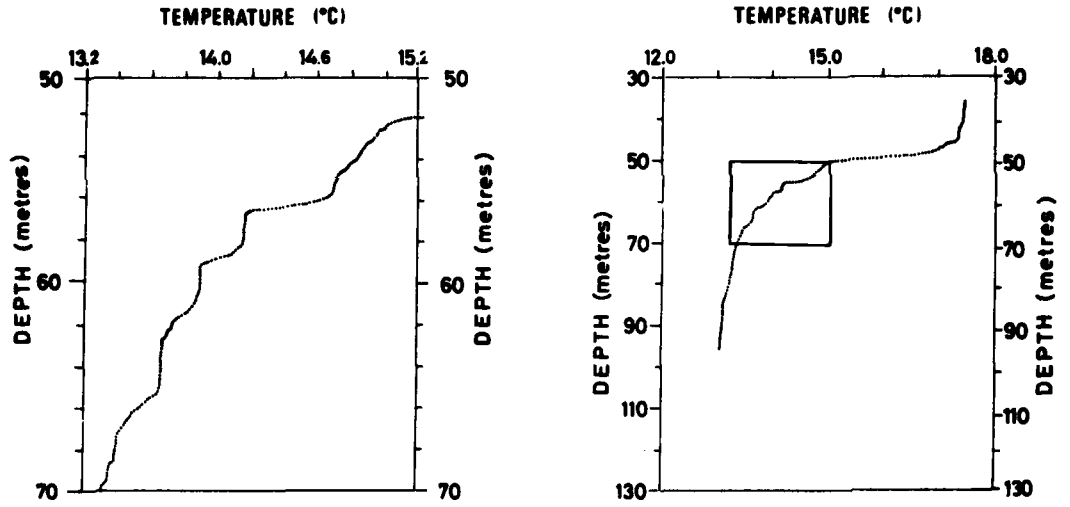


*FIG. 13 FINE STRUCTURE IN TYPICAL TEMPERATURE PROFILE*

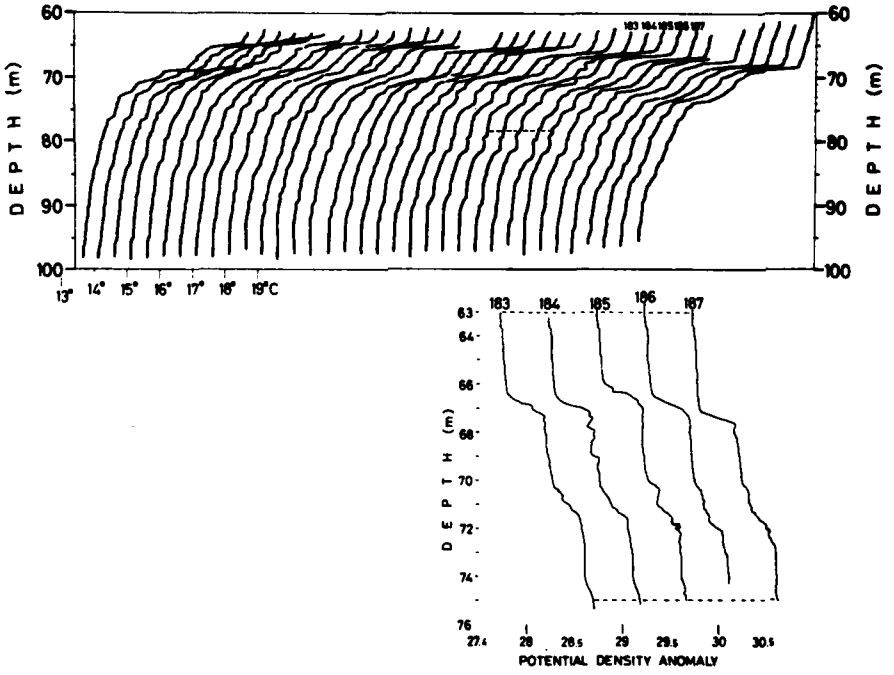


*FIG. 14 TEMPERATURE PROFILE SERIES SHOWING DOWNWARD MOTION AND TWO REGIONS OF HIGH TEMPERATURE GRADIENTS*

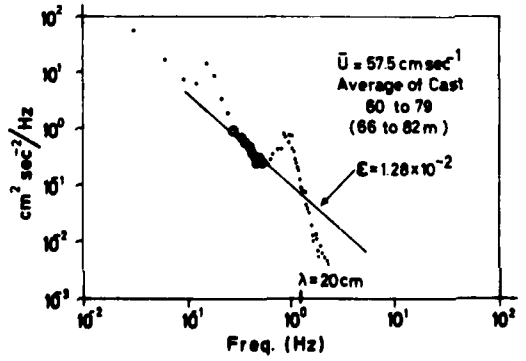


*FIG. 15*
*TYPICAL SPECTRUM OF CURRENT DATA*

Figure 16 shows a typical Väisälä-Brunt frequency profile obtained in our experiments. Initially, an attempt was made to obtain b and No by fitting the N(z) data to Eq. 5. However, the moored current-meter spectra, the horizontal wavenumber tow spectra, and the vertical wavenumber profiling spectra could not be reconciled with the Garrett-Munk models, even if E were left as a free parameter. But, by adopting their suggested values of b=1300 m and No=3 cycle/h, all three spectra were found to be consistent with their models. The resulting free-fit value of E was a factor of 3 below their value. This value of $2.5 \times 10^{-5}$ is also close to Perkin's *[14]* average value of $1.8 \times 10^{-5}$ for the western Mediterranean.

As seen earlier, for the vertical and horizontal wavenumber power spectra of isopotential density surface fluctuations, the *GM75* model predicts a $(\text{wavenumber})^{(-5/2)}$ for large wavenumbers, while Cairns and Williams *[15]* predict a $(\text{wavenumber})^{(-2)}$ form. The horizontal wavenumber spectra (Figs. 8 and 12) do not have enough degrees of freedom to distinguish between the two, although they favour the -2 form. However, the vertical wavenumber spectra (Fig. 11) do support the *GM75* form. For wavelengths shorter than 30 cm, we find a change in slope to $(\text{wavenumber})^{(-5/3)}$, which is believed to be due to turbulence and not to internal waves.

## 3.6 Acoustic Data

The transmitted signal, see Fig. 2a, was a short pulse containing energy at from 3 to 12 kHz. This made identification of different arrivals easier, and avoided the additional interpretational problems of amplitude fluctuations caused by different rays constructively and destructively interfering with one another. In addition, easier identification was possible for arrivals that had suffered a $\pi/2$ phase shift by refraction in the thermocline *[16]*. Figure 2b shows a refracted signal, which can often be identified in the time history of a hydrophone signal. Figure 17 displays the signals of every 50th ping from one hydrophone (data were collec ted at 1 ping per second) aligned by a time shift corresponding to the time of maximum cross-correlation between the nth ping and the (n+1)th ping. Run 13 collected data for 4 ms, while run 28 took data for 8 ms per ping. All the runs, covering 3 to 10 km, had multiple arrivals, as shown in the figure. However, the 1975 test cruise collected some data at 300 to 500 m ranges, and although the data were not of high quality, due to equipment problems, multiple arrivals were observed not to occur at those short ranges.

In order to attempt to separate the various arrivals and examine their amplitude and vertical angle-of-arrival histories, a novel processing technique was developed. The first ping of a run was studied and assigned a fixed number of arrivals within that ping. A least-squares fit with a sum of replicas of the signal was made by varying the amplitude and time of arrival of each replica arrival until a minimum in the residual was obtained (the residual is the difference between the actual data and the set of adjusted replicas). The amplitudes and time of arrivals were further interpolated and recorded, as well as used for initiation of the next ping's fit. In this manner, a time series of amplitudes and arrival times was generated for each hydrophone and for each arrival.

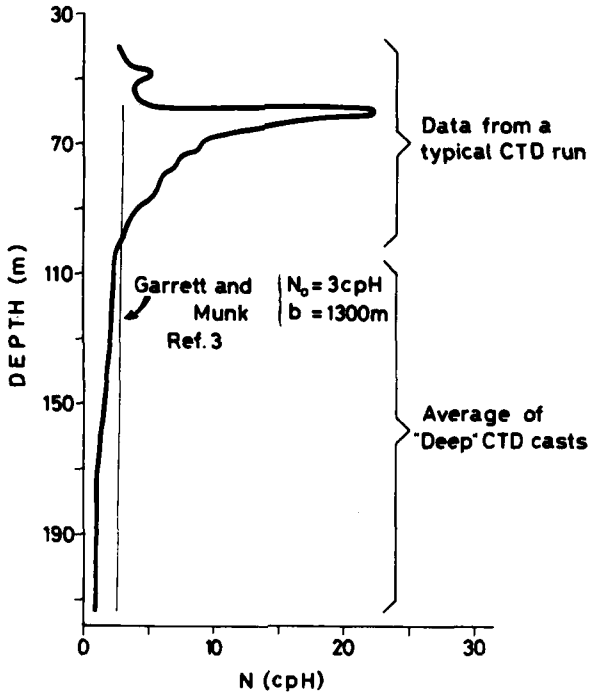


*FIG. 16 TYPICAL VAISALA-BRUNT PROFILE COMPARED WITH GM MODEL*

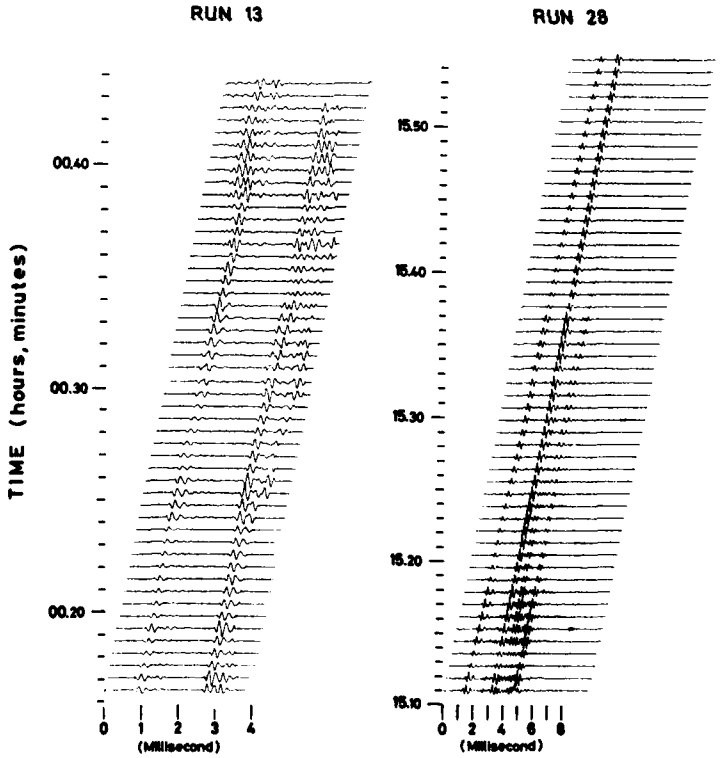


*FIG. 17 SIGNALS FROM SINGLE HYDROPHONE*

A time history of 4096 pings for run 13 is shown in Fig. 18 for four arrivals of hydrophone 1. The different paths were identified by computing the vertical angles of arrivals from the difference in arrival times between hydrophones. However, variations in arrival angle are partially due to array motion. We have therefore used the first arrival, which was the most direct path, as a reference, and have computed angles of arrival with respect to this. Figure 19 shows the time history of this relative angle of arrival for the first 2048 pings of run 13. Ping-to-ping variations of arrival time were quite small, about 2 μs rms, when processed in this manner. With this precision, the arrival angles have apparent beam widths that are two orders of magnitude narrower than those obtainable by means of conventional beamforming.

## SUMMARY AND CONCLUSIONS

### Internal Waves and Blobs

In the internal-wave experiment, moored current meter measurements, horizontal tows, and repeated vertical profiles were made to describe the internal wave field and to compare data from the Mediterranean with the internal 1975 wave model of Garrett and Munk (*GM75*). We found that the energy level, as described by the parameter E, is a factor of 3 lower than the model's value of $6.3 \times 10^{-5}$. We also found that appropriate values of b, the vertical stratification scale, and No, the maximum stability frequency, could not be established by simply fitting measured values of N(z) to an exponential function. By using the values suggested by the authors for deep oceans, however, agreement was obtained between the model and our data. The form of the vertical wavenumber spectra at high wavenumbers fits a $(\text{wavenumber})^{-5/2}$, agreeing with *GM75* and contrasting with $(\text{wavenumber})^{-2}$ of Cairns and Williams *[15]*, and Desaubies *[17]*. The shape of the horizontal wavenumber spectrum however, is better fitted by a $(\text{wavenumber})^{-2}$ form, although more uncertainty exists in these data due to the reduced number of degrees of freedom for horizontal data. From analyses of temperature and density data, non-propagating horizontal features, or blobs, were found to be lacking in this experimental setting.

Inertial motions dominate the vertical shear in the thermocline, with longer-period motions and the shorter-period internal waves contributing only a small fraction to the shearing. One large-scale event that appeared to drastically alter the thermal structure of the thermocline was observed. This event appeared to cause complete mixing of the thermocline, and it had many of the characteristics of laboratory-generated solitary waves.

### Microstructure and Turbulence

A common characteristic of the fine-scale vertical feature was the presence of sheets and layers, which appeared not to be internal waves as such, but rather to be riding up and down with the internal waves. Fine-scale mixing events were observed during 1 to 2% of the time;

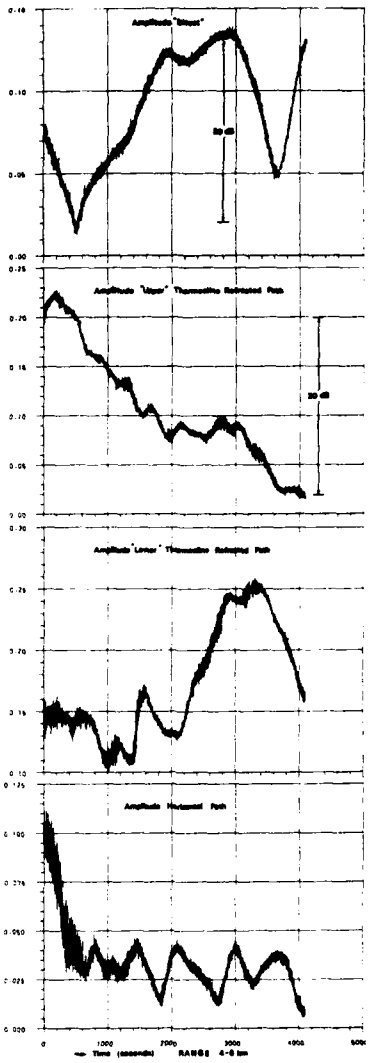

*FIG. 18 TIME HISTORIES OF PINGS RECEIVED AT SINGLE HYDROPHONE ALONG FOUR DIFFERENT PATHS*

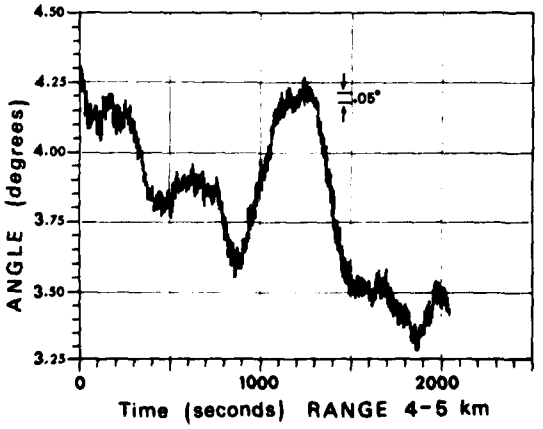


*FIG. 19 TIME HISTORY OF VERTICAL ARRIVAL ANGLE (Upper Thermocline Refracted Path)*

these had relatively large rates of dissipation of kinetic energy, $\varepsilon$, of about 0.2 to 1.0 $cm^2 s^{-3}$. Spectral analysis of the current-meter data gave an average value of $\varepsilon$ of about $1 \times 10^{-2}$ $cm^2 s^{-3}$, indicating that this magnitude could be explained by events occurring relatively rarely and suggesting an intermittent turbulent field.

The vertical wavenumber spectra of temperature and density shows a wavenumber$^{-5/3}$ form for wavenumbers larger than about 3 cycle/m, consistent with turbulence theories.

## Acoustic Propagation

Short pulses were transmitted to a five-element vertical array on the receiving vessel, which was drifting over a range of 3 to 10 km from the source. A technique was devised whereby arrivals from different vertical directions could be followed, forming a time or space series of their amplitudes and their times of arrival. Usually a particular vertical arrival could not be followed over as much as 5 km, due to its fading. Short-term fluctuations of the vertical angles of arrival were of the order of 0.02° rms over the four-wavelength array, yielding resolution far in excess of both conventional beamforming and the higher-resolution maximum-likelihood method. Large amplitude fluctuations (>20 dB) of a particular arrival were observed. The time spread of the different arrivals was as much as 5 ms.

The multiplicity of arrivals and their fluctuations may be due to microstructure or internal waves or, more likely, to a combination of both. While range-independent ray tracings incorporating step profiles show the proper number of arrivals, they do not reveal all the features observed. It seems clear that range-dependent modelling investigations are necessary to separate and to clearly understand the individual effects of microstructure, turbulence, and internal waves.

## ACKNOWLEDGMENTS

The SACLANT ASW Research Centre wishes to acknowledge the contribution of the French Navy in arranging for the use of the BOHRA II moored buoy and of the Italian Navy in providing the services of its Hydrographic Ship MAGNAGHI. It thanks to the personnel of these units for their participation.

The following members of SACLANTCEN made particular contributions:

| | |
|---|---|
| G. Pranzo Zaccaria: | Analysis of the acoustic signals. |
| Oceanographic Instrumentation Dpt: | Development of the Towed Oscillating Body. |

## REFERENCES


1. GARRETT, C.J.R. and MUNK, W.H. Space-time scales of internal waves. *Jnl Geophysical Fluid Dynamics* 2, 1972: 225-264.

2. BRISCOE, M.G. Internal waves in the ocean. *Reviews of Geophysics and Space Physics* 13(3), 1975: 591-645.

3. GARRETT, C.J.R. and MUNK, W.H. Space-time-scales of internal waves: a progress report. *Jnl Geophysical Research* 3, 1975: 291-297.

4. OSBORN, T.R. and COX, C.S. Oceanic fine-structure. *Geophysical Fluid Dynamics* 3, 1972: 321-345.

5. GARRETT, C.J.R. and MUNK, W.H. Oceanic mixing by breaking internal waves. *Deep Sea Research* 19, 1972: 823-832.

6. GIBSON, C.H., VEGA, L. and WILLIAMS, R.B. Diffusion of heat and momentum in the oceans. *In:* LANDSBERG, H.E. *ed.* Advances in Geophysics, Vol 18A. New York, N.Y., Academic Press, 1974.

7. WILLIAMS, R.B. and GIBSON, C.H. Direct measurements of turbulence in the Pacific equatorial undercurrent. *Jnl Physical Oceanography* 4, 1974: 104-108.

8. CHERNOV, L. Wave Propagation in a Random Medium. New York, N.Y., McGraw-Hill, 1960.

9. TATARSKI, V.I. The effects of the turbulent atmosphere on wave propagation. Translated from the Russian. Jerusalem, Israel, Program for Scientific Translation, 1971.

10. PORTER, R.P., SPINDEL, R.C. and JAFFEE, R.J. Acoustic internal wave interaction at long ranges in the ocean. *Jnl Acoustical Society America* 56, 1974: 1426-1436.

11. FLATTE, S.H. and TAPPERT, F.D. Calculation of the effect of internal waves on oceanic sound transmission. *Jnl Acoustical Society America* 58, 1975: 1151-1159.

12. MUNK, W.H. and ZACHARIASEN, F. Sound propagation through a fluctuating stratified ocean: theory and observation. *Jnl Acoustical Society America* 59, 1976: 818-838.

13. DE STROBEL, F. et al. New oceanographic tools at SACLANTCEN, (NATO UNCLASSIFIED). *In*: SACLANTCEN. Papers presented to the 29th meeting of the SACLANTCEN Scientific Committee of National Representatives 2-4 Nov 1976, NATO CONFIDENTIAL. La Spezia, Italy, SACLANT ASW Research Centre, 1976: pp 8-1 to 8-4. *[AD CO 10187]*

14. PERKINS, H.T. Inertial oscillations in the Mediterranean. (thesis) M.I.T. and W.H.O.I., 1970.

15. CAIRNS, J.L. and WILLIAMS, G.O. Internal wave observations from a midwater float, 2. *Jnl Geophysical Research* 81(12), 1976: 1943-1950.

16. BARASH, R.M. Evidence of phase shift at caustics. *Jnl Acoustical Society America* 43(2), 1968: 378-380.

17. DESAUBIES, Y.J.F. Analytical representation of internal wave spectra. *Jnl Physical Oceanography* 6, 1976: 976-981.

*(NOTE: Documents with AD numbers may be obtained from the US National Technical Information Service or national outlets in other nations.)*